https://doi.org/10.5194/egusphere-2026-7013
Preprint. Discussion started: 20 November 2026
© Author(s) 2026. CC BY 4.0 License.

Long-term responses of sediment nitrogen cycling to environmental change in a semi-enclosed inland sea

Zhaosen Wu [1], Xinyu Guo [2, *], Masatoshi Nakakuni [3, 4], Kuninao Tada [3, 4]

[1]Key Laboratory of Marine Environment and Ecology, Ministry of Education of China, Ocean University of China, 238 Songling Road, Qingdao 266100, China

[2]Center for Marine Environmental Studies, Ehime University, 2-5 Bunkyo-Cho, Matsuyama 790-8577, Japan

[3]Faculty of Agriculture, Kagawa University, Ikenobe, Kita, Miki, Kagawa 761-0701, Japan

[4]Seto Inland Sea Regional Research Center, Kagawa University, Saiwai, Takamatsu, Kagawa 761-0016, Japan

* Corresponding Author: **Xinyu Guo** - Center for Marine Environmental Studies, Ehime University, 2-5 Bunkyo-Cho, Matsuyama 790-8577, Japan; Email: guo.xinyu.mz@ehime-u.ac.jp; ORCID: 0000-0002-4832-8625

Abstract. Sediment nitrogen cycling regulates nutrient retention, ecosystem functioning, and greenhouse gas emissions in coastal seas. However, its response to long-term environmental change and the underlying drivers remain poorly understood because of limited long-term observations. Using Harima Nada as a study system, we combined multi-decadal monitoring data with a one-dimensional sediment model to reconstruct sediment nitrogen cycling and sediment–water nitrogen fluxes from 1992 to 2021. We show that interannual variations in sediment nitrogen cycling are driven by changes in organic matter deposition, its degradability, microphytobenthos activity, and oxygen-dependent nitrogen transformations. Attribution experiments further reveal that eutrophication recovery substantially alters sediment nitrogen cycling by reducing particulate organic nitrogen inputs, whereas nitrogen accumulated during eutrophic periods is gradually recycled to the overlying water as benthic dissolved inorganic nitrogen fluxes. Consequently, the magnitude and persistence of sediment nutrient legacy effects are determined by the intensity and duration of eutrophication. In contrast, seawater warming exerts only negligible effects on sediment nitrogen cycling over decadal timescales. These findings establish a process-based attribution framework for evaluating the impacts of long-term sediment nitrogen dynamics, identifying eutrophication rather than seawater warming as the dominant driver and highlighting the importance of sediment legacy effects for coastal nutrient management.

https://doi.org/10.5194/egusphere-2026-7013
Preprint. Discussion started: 20 November 2026
© Author(s) 2026. CC BY 4.0 License.



Keywords: Sediment nitrogen cycling, Benthic nutrient flux, Long-term environmental change, Eutrophication recovery, Seawater warming

https://doi.org/10.5194/egusphere-2026-7013
Preprint. Discussion started: 20 November 2026
© Author(s) 2026. CC BY 4.0 License.

1 Introduction

Coastal nitrogen cycling plays a critical role in regulating nutrient availability, primary production and greenhouse gas emissions (Devol, 2015; Han et al., 2021). Especially in semi-enclosed inland seas, limited exchange with the open ocean and strong anthropogenic forcing makes coastal ecosystems susceptible to eutrophication, hypoxia, and long-term regime shifts (Diaz and Rosenberg, 2008; Ding et al., 2023). As the major reservoir of particulate organic nitrogen (PON), sediments store deposited organic matter, regenerate dissolved inorganic nitrogen (DIN), and permanently remove reactive nitrogen through denitrification and anammox (Boynton et al., 2017; Huang et al., 2021). Because sediment nitrogen cycling integrates environmental changes over longer timescales than the overlying water, understanding its long-term response is essential for predicting coastal ecosystem trajectories and informing nutrient management.

Coastal environments have experienced concurrent eutrophication and seawater warming over recent decades, both of which can alter sediment biogeochemistry by modifying organic matter deposition, oxygen availability, and microbial nitrogen transformations (Dai et al., 2023; Pörtner et al., 2019). However, sediment nitrogen responses at interannual to decadal timescales remain poorly understood. Previous studies have largely focused on seasonal variability in sediment nutrient concentrations, benthic fluxes, and nitrogen transformation rates, whereas longer-term studies have primarily relied on sediment archives to reconstruct millennial-scale environmental changes (Ding et al., 2021; Oliver et al., 2010). The scarcity of long-term observations has limited efforts to resolve how sediment nitrogen cycling responds to environmental changes and to distinguish the effects of concurrent environmental drivers. This distinction is particularly important because sediments can retain and gradually regenerate organic and inorganic nitrogen, producing legacy effects and delayed responses to changes in external nutrient loading (Lønborg and Markager, 2021; Soetaert and Middelburg, 2009).

Harima Nada, in the eastern Seto Inland Sea of Japan, provides an opportunity to address this challenge (Leng et al., 2023). Over recent decades, this semi-enclosed coastal sea has experienced a substantial reduction in nutrient loading following eutrophication control alongside persistent seawater warming, resulting in concurrent anthropogenic and climatic changes in its biogeochemical environment (Ishii et al., 2014; Nakakuni et al., 2026; Yamamoto et al., 2021). Long-term observations of bottom-water and

https://doi.org/10.5194/egusphere-2026-7013
Preprint. Discussion started: 20 November 2026
© Author(s) 2026. CC BY 4.0 License.

sediment conditions provide a unique opportunity to investigate sediment responses to these concurrent environmental changes and to distinguish their relative influences.

In this study, we apply a one-dimensional sediment nitrogen model constrained by long-term observations in Harima Nada to investigate the interannual evolution of sediment nitrogen cycling from 1992 to 2021. We (1) quantify long-term variations in sediment nitrogen inventories and sediment–water nitrogen fluxes, (2) identify the dominant environmental drivers using process-based attribution experiments, and (3) separately evaluate the influences of eutrophication recovery and seawater warming using a normalized impact assessment. By distinguishing these concurrent environmental influences, this study provides a process-based framework for understanding long-term sediment nitrogen dynamics in semi-enclosed coastal seas and offers insights into nutrient management strategies that account for sediment legacy effects under future environmental change.

2 Materials and Methods

2.1 Study area

Harima Nada is located in the eastern Seto Inland Sea, Japan, with a mean water depth of approximately 26 m (Figure 1). It is connected to Osaka Bay to the east and Hiuchi Nada to the west., while exchange with the Pacific Ocean occurs through the Naruto Strait and the Kii Channel located to the south (Zhu et al., 2019). The hydrographic environment exhibits pronounced seasonal variability driven by wind forcing and density stratification (Tong-u-dom et al., 2023). During winter, prevailing northwesterly winds generate a predominantly wind-driven circulation pattern, whereas in summer a density-driven cyclonic circulation develops in response to spatial gradients in stratification. The water column is strongly stratified during the warm season, leading to the formation of bottom cold water, while it is vertically homogeneous during winter due to strong mixing. These seasonal hydrographic changes regulate the temperature, oxygen, and nutrient conditions experienced by the seafloor.

The Seto Inland Sea experienced severe eutrophication during the 1960s and 1970s following rapid industrialization and urbanization. In response, the Japanese government implemented a series of environmental management policies beginning in the 1970s to reduce nutrient loading and improve water

https://doi.org/10.5194/egusphere-2026-7013
Preprint. Discussion started: 20 November 2026
© Author(s) 2026. CC BY 4.0 License.

quality (Ishii et al., 2014; Yamamoto et al., 2021). The Seto Inland Sea experienced severe eutrophication during the 1960s and 1970s following rapid industrialization and urbanization. A series of environmental management measures implemented since the 1970s substantially reduced nutrient loading and gradually shifted the system toward less nutrient-enriched conditions. More than four decades of seasonal monitoring by the Japanese Ministry of the Environment show that total nitrogen concentrations increased until the mid-1990s and subsequently declined, while summer bottom-water DO improved after 2010 (https://water-pub.env.go.jp/water-pub/mizu-site/mizu/kouiki/dataMap.asp) (Figure S1a,b). In contrast, chlorophyll-a concentrations remained relatively stable, with a slight increasing trend (Figure S1c). Seawater temperature exhibits a pronounced seasonal cycle and a long-term warming trend, particularly during autumn and winter (Figure S1d). These concurrent changes in nutrient availability, oxygen conditions, and temperature provide an environmental context for assessing long-term changes in sediment nitrogen cycling.

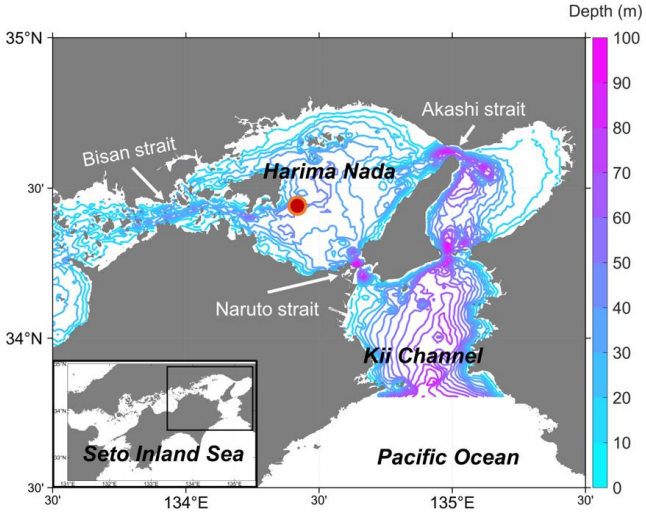


Figure 1. Study area of the Harima Nada in the Seto Inland Sea, Japan. The red dot represents the site where the observational data used in this study were collected.

The seafloor of Harima Nada is dominated by fine-grained muddy sediments, with mud contents generally exceeding 70 % (Yamaguchi et al., 2014), supporting diverse and abundant macrobenthic communities (Tsujino, 2018). Sediment properties, including grain-size composition, organic matter

https://doi.org/10.5194/egusphere-2026-7013
Preprint. Discussion started: 20 November 2026
© Author(s) 2026. CC BY 4.0 License.

content, and redox conditions, strongly regulate benthic community structure and ecosystem functioning in this region (Nishijima et al., 2015). Through bioturbation, bioirrigation, and organic matter processing, benthic organisms actively modify sediment biogeochemical processes and nutrient transformations. Furthermore, sediment-derived DIN fluxes have been reported to be comparable in magnitude to riverine DIN inputs, highlighting the importance of sediment-water exchanges as an internal nutrient source for the ecosystem (Leng et al., 2023; Nakakuni et al., 2024).

2.2 Field sampling and measurements

Sediment observations used in this study were obtained at Site NH (34°28.00′N, 134°24.00′E) in Harima Nada. Sediment samples collected during the early 1990s and the period of 2019–2021 were used to characterize long-term changes in sediment nitrogen profiles. The datasets included solid-phase PON concentrations and pore-water DIN concentrations. Specifically, pore-water NH_4^+ profiles were available for 1992–1993 and 2020–2021, while pore-water NO_x^- (NO_2^-+NO_3^-) profiles were available only for 2020–2021.

Sedimentary PON profiles for the early 1990s were obtained at Site NH from published observations (Ichimi et al., 2005). Pore water for 1992 and 1993, in contrast, was obtained from sediment cores collected at Site NH and processed following the methods of Tada and Montani (Tada and Montani, 1997), as detailed below. The core samples were collected using a K.K. (Kawai, Kyoto University)-type gravity corer with 50 cm long acrylic pipe, 4 cm in diameter (Hashimoto Kagaku Co.). Pore waters were separated from the solid phase by centrifugation at 3000 r.p.m. for 15 min. after cutting core samples into 0.5 – 2.0 cm sections. The supernatant was filtered through pre-combusted (450℃ for 4h) Whatman GF/F filters. All procedures were carried out in a few hours. The pore water samples were stored at -20℃ until chemical analysis. Nutrient concentrations in the pore water were determined with a Technicon Autoanalayzer II (Technicon Co., USA), following standard analytical methods (Strickland and Parsons).These pore-water DIN profiles for the early 1990s are previously unpublished and were provided by the database of the Seto Inland Sea Regional Research Center, Kagawa University.

Sediment cores were collected at Site NH during four cruises in July 2019, August 2020, November 2020, and April 2021 using a G.S. type core sampler “Asyura” (Rigo Co., Tokyo, Japan), and were sectioned at 1-cm intervals immediately after retrieval. For sedimentary PON profiles, each section was stored

https://doi.org/10.5194/egusphere-2026-7013
Preprint. Discussion started: 20 November 2026
© Author(s) 2026. CC BY 4.0 License.

frozen, then freeze-dried. The dried samples were thoroughly homogenized using a mortar and pestle, and carbonates were removed by treatment with 1 M hydrochloric acid (HCl) (Hedges and Stern, 1984). The decarbonated sediment powders were sealed in tin capsules, and PON concentrations were determined for samples collected in October 2020 using an elemental analyzer (CHN coder; JM10, J-Science Lab, Kyoto, Japan). Pore-water DIN concentrations (NH_4^+ and NO_x^-) were obtained from the same cores for 2019–2021 and measured following the analytical procedures described by a previous study (Nakakuni et al., 2024). These 2019–2021 profiles are previously unpublished and were provided by the database of the Seto Inland Sea Regional Research Center, Kagawa University.

2.3 Model description

A one-dimensional vertical sediment biogeochemical model was developed to simulate nitrogen cycling and sediment–water exchanges in Harima Nada. The model follows the reaction–transport framework for early diagenesis (Berner, 1980) and was further developed and applied in our previous study (Wu et al., 2026).

The model consists of solid and pore-water phases and includes two PON pools with different degradabilities, together with DO, ammonium (NH_4^+), nitrite (NO_2^-), nitrate (NO_3^-), and oxygen demand units (ODU) in the pore-water phase. A surface fluff layer is included to represent rapid benthic recycling and exchange with the overlying water.The model resolves the major pathways of sediment nitrogen cycling, including PON mineralization, nitrification, denitrification, anaerobic ammonium oxidation (anammox), and dissimilatory nitrate reduction to ammonium (DNRA), together with transportations by burial, molecular diffusion, bioturbation, bioirrigation, particle sinking, and resuspension. Sediment–water exchanges of solutes are calculated by Fick's First law, whereas particulate organic matter exchange is regulated by sea bottom stress.

The model domain extends from the sediment surface to the underlying sediment layers and is forced by observed bottom-water conditions, including temperature, bottom stress, DO, PON, and DIN concentrations. This framework allows temporal variations in overlying-water conditions to propagate through sediment biogeochemical processes and ultimately affect benthic nitrogen fluxes. Detailed model equations, parameterizations, boundary conditions, and numerical implementation are provided in Supplementary Material Text S1.

https://doi.org/10.5194/egusphere-2026-7013
Preprint. Discussion started: 20 November 2026
© Author(s) 2026. CC BY 4.0 License.

2.4 Model and simulation configurations

The model domain comprises the upper 10 cm of sediment, which was evenly divided into 100 layers to resolve the vertical concentration profiles of key nitrogen components. The simulation covered the period from July 1992 to April 2021.

The initial conditions for the state variables were specified based on sediment observations at Station NH. Initial profiles of PON and NH_4^+ were prescribed from observations conducted in 1990 and July 1992, respectively. Because the concentrations of DO, NO_2^- and NO_3^- were unavailable at the same time, their initial profiles were taken from observations in 2000 (Sayama et al., 2002) and July 2020. The initial concentration of ODU was uniformly set to 100 mmol m^{-3} and allowed to evolve dynamically thereafter. The porosity profile measured in 2020 was prescribed as a consistent input condition throughout the simulation (Text S2 and Figure S4). The study site is characterized by muddy sediments. Given the extended spin-up period, model results were largely insensitive to the prescribed initial profiles.

Monthly bottom-water temperature and concentrations of PON, NH_4^+, NO_2^-, NO_3^-, and DO from 1992 to 2021 (Figures 2a–f) were interpolated from quarterly monitoring data provided by the Japanese Ministry of the Environment and prescribed as upper-boundary conditions at the sediment–water interface. Hourly bottom stress (Figure 2g) was extracted from a three-dimensional hydrodynamic model simulation that reproduces the seasonal circulation of the Seto Inland Sea (Leng et al., 2023). At the lower boundary of model domain, NH_4^+ and NO_2^- concentrations beneath the model domain were fixed at their initial values. Because NO_3^- and DO were assumed absent in the underlying deep anoxic sediments, no diffusive exchange across the lower boundary was allowed, and their bottom-boundary fluxes were therefore set to zero. The ODU concentration was set to 0 mmol m^{-3} in the overlying water and fixed at 100 mmol m^{-3} beneath the model domain (Soetaert et al., 1996).

To reproduce the observed interannual variability in sedimentary PON profiles, a time-varying annual sediment mineralization rate was prescribed (Figure 2h). The mineralization rates were estimated from an independent decadal observational dataset provided by the Japanese Ministry of the Environment and further refined through model sensitivity analyses (Text S3 and Figure S5). This parameterization represents temporal variations in the degradability of deposited organic matter and the activity of microphytobenthos. The prescribed long-term trend is consistent with observed changes in

https://doi.org/10.5194/egusphere-2026-7013
Preprint. Discussion started: 20 November 2026
© Author(s) 2026. CC BY 4.0 License.

phytoplankton and microphytobenthos abundances and community composition in Harima Nada (Itakura and Yamaguchi, 2007; Nishikawa et al., 2009). Both groups declined during the 1980s, continued decreasing more gradually through the 1990s, increased during the 2000s, and decreased again after the late 2010s (Figure S6). During this period, the dominant species shifted from *Skeletonema* to *Chaetoceros*, with the former generally producing more labile detritus than the latter (Itakura and Yamaguchi, 2007; Nishikawa et al., 2009).

To obtain a stable initial state, the model was first spun up under repeated 1992 forcing conditions until equilibrium was reached. The transient simulation was then performed from July 1992 to April 2021 using the time-varying forcing described above.

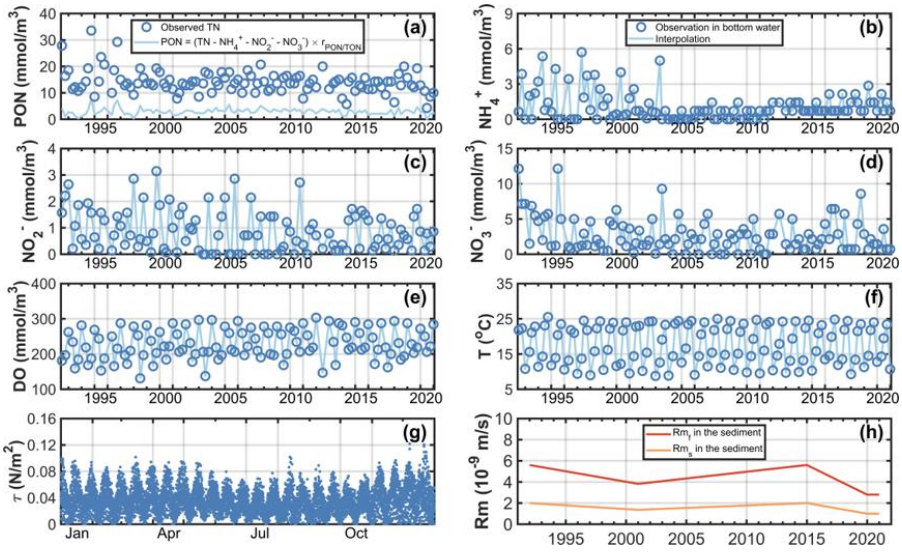


Figure 2. Input conditions of the sediment model: (a) PON concentration, (b) NH_4^+ concentration, (c) NO_2^- concentration, (d) NO_3^- concentration, (e) DO concentration, (f) temperature in the bottom water, (g) bottom stress and (h) sedimentary mineralization rate for fast-decaying PON (Rm_f) and slow-decaying PON (Rm_s). The proportion of PON relative to total organic nitrogen ($r_{PON/TON}$) in the bottom water is derived from a previous study of this sea area (Hayashi, 2001).

2.5 Model validation

To evaluate model performance, simulated sediment nitrogen concentrations were compared with observations collected during two periods, July 1992–January 1993 and July 2019–April 2021 (Figure 3). The model successfully reproduced both the seasonal variability and the pronounced differences in sediment nitrogen profiles between the early 1990s and 2019–2021.

https://doi.org/10.5194/egusphere-2026-7013
Preprint. Discussion started: 20 November 2026
© Author(s) 2026. CC BY 4.0 License.

For PON, the model captured the substantially higher concentrations observed in 2020 compared with those in the early 1992 (Figures 3a, c). Simulated NH_4^+ concentrations exhibited overall agreement with seasonal observations in both periods, reproducing both the observed concentration range and vertical gradients throughout the sediment column (Figures 3b, d). For NO_3^-, the model generally captured the observed concentration ranges, seasonal trends, and depth-dependent distribution, despite some mismatches in concentration values at individual depths and sampling times (Figure 3e).

Overall, the model reproduced not only the seasonal evolution of sediment nitrogen profiles but also the marked interannual differences between the early 1990s and 2019–2021. These results indicate that the model captures the dominant processes governing sediment nitrogen cycling in Harima Nada and is therefore suitable for investigating long-term changes in sediment–water nitrogen exchange.

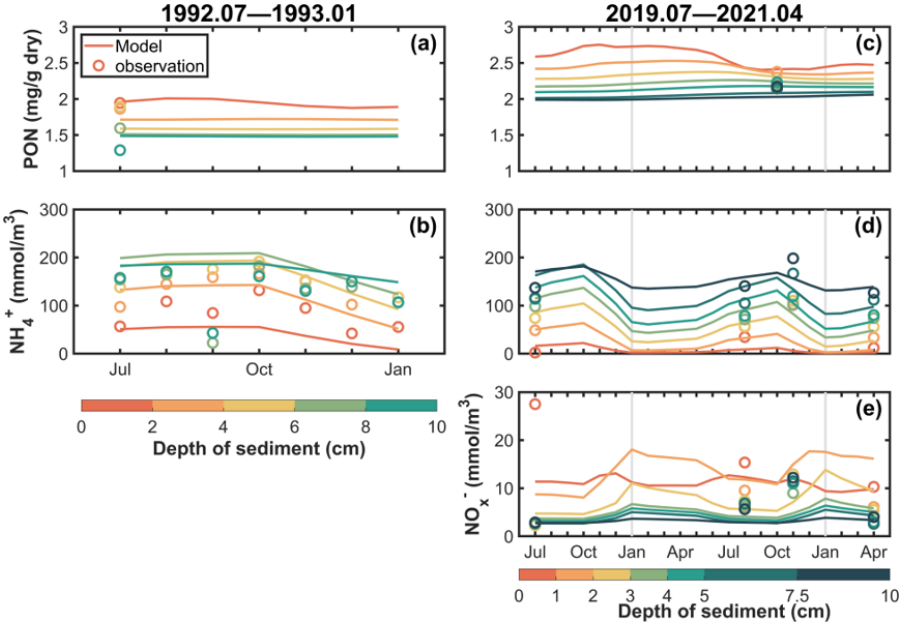


Figure 3. Comparison between observed and simulated concentrations of PON (a, c), NH_4^+ (b, d), and NO_x^- (e) at different sediment depths during July 1992–January 1993 (a, b) and July 2019–April 2021 (c–e). Lines represent model results and circles represent observations. Colors indicate sediment depth.

https://doi.org/10.5194/egusphere-2026-7013
Preprint. Discussion started: 20 November 2026
© Author(s) 2026. CC BY 4.0 License.

3 Results

3.1 Interannual variations in sediment biogeochemical profiles

The TN concentration in the Harima Nada sediments increased over the past three decades (Figure S7). It rose from approximately 1.65 mg g^{-1} in the early 1990s to a peak of 2.31 mg g^{-1} around 2010, and then fluctuated slightly while remaining close to 2.2 mg g^{-1} thereafter. This long-term increase was consistent in both magnitude and trend with independent observational datasets (Kamiyama et al., 1998; Nakakuni et al., 2022; Yamaguchi et al., 2014) as well as observations archived in the Seto Inland Sea Comprehensive Water Quality Survey database (https://www.pa.cgr.mlit.go.jp/suishitu/), and was primarily associated with the accumulation of PON.

PON concentrations increased gradually over time at all sediment depths while maintaining a persistent vertical gradient, with concentrations decreasing away from the sediment surface (Figure 4a). The surface layer exhibited the largest interannual variability, increasing from 1.85 mg g^{-1} in 1993 to 2.73 mg g^{-1} in 2008, declining to 2.29 mg g^{-1} in 2017, and then recovering to 2.51 mg g^{-1} by 2020. The magnitude of temporal variation decreased with sediment depth. In the deepest layer, PON concentrations increased steadily from approximately 1.50 mg g^{-1} in the early 1990s to around 2.05 mg g^{-1} during the 2010s, indicating progressive accumulation of organic nitrogen throughout the sediment column.

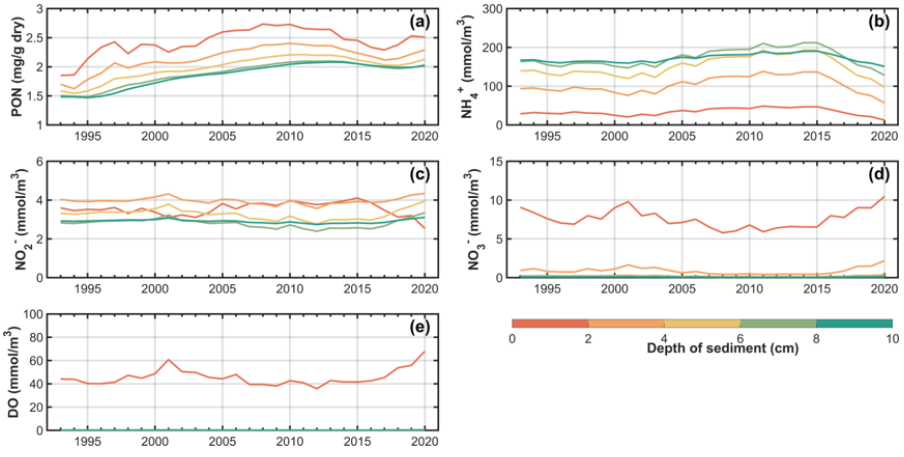


Figure 4. The interannual variations of annual mean concentration profiles of (a) PON, (b) NH_4^+, (c) NO_2^-, (d) NO_3^- and (e) DO in different layers in the sediment from 1993 and 2020.

NH_4^+ concentrations increased markedly with sediment depth, with the surface layer exhibiting the lowest concentrations and the smallest interannual variability (12.38–48.74 mmol m^{-3}) (Figure 4b).

https://doi.org/10.5194/egusphere-2026-7013
Preprint. Discussion started: 20 November 2026
© Author(s) 2026. CC BY 4.0 License.

Concentrations increased rapidly between 2 and 8 cm, where the largest temporal variations appeared. Between 2004 and 2017, the maximum NH_4^+ concentrations occurred at 6–8 cm rather than in the deepest (8–10 cm) layer, reaching a peak of 211.96 mmol m^{-3}. In contrast, concentrations in the deepest layer varied only modestly (150.79–190.17 mmol m^{-3}). Across all depths, NH_4^+ concentrations increased gradually from 1993, peaked between 2011 and 2015, and subsequently declined toward 2020, resulting in observations of vertical concentration profiles in 2020 that were similar to those in 1993 (Figure 3b, d).

NO_2^- concentrations were much lower than NH_4^+ concentrations and exhibited only limited interannual variability (Figure 4c). The highest NO_2^- concentrations consistently occurred in the 2–4 cm layer, remaining close to 4 mmol m^{-3} throughout the study period. Concentrations in deeper sediments gradually decreased with depth and generally remained between 3 and 4 mmol m^{-3}. Pronounced interannual variation was observed only in the surface layer, where NO_2^- increased from 3.60 mmol m^{-3} in 1993 to 4.11 mmol m^{-3} in 2015 before decreasing rapidly to 2.54 mmol m^{-3} in 2020.

NO_3^- was restricted to the sediment surface, whereas concentrations below 2 cm remained close to zero throughout the study period (Figure 4d). Surface NO_3^- concentrations exhibited pronounced interannual variability, decreasing from 9.08 mmol m^{-3} in 1993 to 6.90 mmol m^{-3} in 1997, increasing to a maximum of 9.79 mmol m^{-3} in 2001, declining again to a minimum of 5.78 mmol m^{-3} in 2008, and finally increasing continuously to 10.47 mmol m^{-3} by 2020.

Similarly, DO was confined to the uppermost sediment layer, while its concentrations below 2 cm remained close to zero throughout the simulation (Figure 4e). Surface DO concentrations increased from 44.14 mmol m^{-3} in 1993 to a peak of 60.78 mmol m^{-3} in 2001, decreased to a minimum of 35.82 mmol m^{-3} in 2012, and then increased steadily to 67.93 mmol m^{-3} by 2020.

Together, these concentration profiles reveal a progressive accumulation of organic nitrogen in the sediment over the past three decades, accompanied by substantial interannual variability in pore-water inorganic nitrogen species, particularly NH_4^+ in the intermediate sediment layers and NO_3^- and DO at the sediment surface.

https://doi.org/10.5194/egusphere-2026-7013
Preprint. Discussion started: 20 November 2026
© Author(s) 2026. CC BY 4.0 License.

3.2 Interannual variations in sediment-water fluxes

The corresponding changes in nitrogen and DO exchange fluxes across the sediment–water interface are shown in Figure 5. The PON flux was consistently directed from the overlying water into the sediment throughout the study period (Figure 5a). It exhibited pronounced interannual variability, fluctuating between 1.35 and 3.78 mmol m^{-2} d^{-1} without a persistent long-term increasing or decreasing trend. Relatively high PON fluxes occurred in the mid-1990s, the mid-2000s, and again in 2019, whereas lower values occurred in the early 2000s, the mid-2010s, and 2020, indicating substantial year-to-year variability in organic nitrogen deposition.

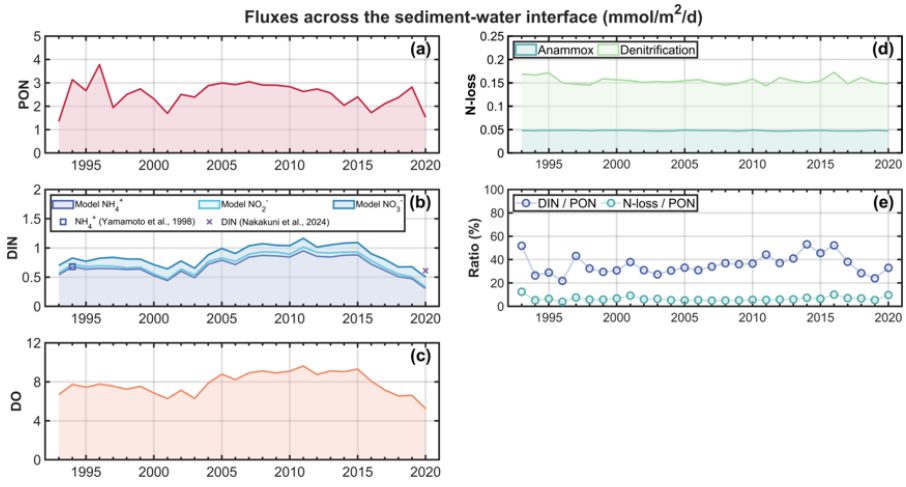


Figure 5. The interannual variations of the fluxes of (a) PON, (b) DIN, (c) DO, (d) N-loss (N_2 and N_2O) at the sediment-water interface, and (e) the ratios of DIN flux and N-loss flux to PON flux. The observational data are obtained from two papers (Nakakuni et al., 2024; Yamamoto et al., 1998).

The DIN flux released from the sediment to the bottom water closed to 0.80 mmol m^{-2} d^{-1} from 1993 to 2003, increased to a maximum of 1.16 mmol m^{-2} d^{-1} in 2011, and subsequently declined to 0.50 mmol m^{-2} d^{-1} by 2020 (Figure 5b). NH_4^+ accounted for 62–85% of the total DIN flux and therefore dominated its interannual variability, ranging from 0.31 to 0.95 mmol m^{-2} d^{-1}. The NO_2^- flux exhibited a similar but much weaker temporal pattern, varying between 0.02 and 0.07 mmol m^{-2} d^{-1}. In contrast, the NO_3^- flux fluctuated between 0.09 and 0.17 mmol m^{-2} d^{-1} without significant interannual variation.

https://doi.org/10.5194/egusphere-2026-7013
Preprint. Discussion started: 20 November 2026
© Author(s) 2026. CC BY 4.0 License.

The DO flux was consistently directed from the overlying water into the sediment and exhibited an interannual pattern similar to that of the total DIN flux (Figure 5c). It increased from 6.69 mmol m^{-2} d^{-1} in 1993 to a maximum of 9.62 mmol m^{-2} d^{-1} in 2011 before decreasing toward 5.24 mmol m^{-2} d^{-1} in 2020. The N-loss flux, representing the production of gaseous nitrogen through denitrification and anammox, remained relatively stable over the past three decades, varying in a small range between 0.14 and 0.17 mmol m^{-2} d^{-1} with no apparent long-term trend (Figure 5d). Denitrification accounted for the majority of the N-loss flux and was the primary source of its limited interannual variability, whereas the anammox flux remained nearly constant at approximately 0.05 mmol m^{-2} d^{-1} throughout the study period.

The DIN:PON and N-loss:PON flux ratios were used to characterize the fractions of deposited PON recycled back to the overlying water and permanently removed from the sediment, respectively (Figure 5e). The DIN:PON flux ratio ranged from 22% to 53%, whereas the N-loss:PON flux ratio varied between 4% and 13%. Both ratios exhibited temporal variations opposite to those of the PON flux, with relatively high values occurring during periods of low PON deposition and vice versa. The sum of the two ratios is always less than 100%, indicating that the sediments in this region exhibited a state of nitrogen storage during the study period.

The contrasting long-term behaviors of nitrogen deposition, recycling, and removal indicate that the pathways regulating sediment nitrogen cycling evolved differently over the past three decades.

4. Discussions

4.1 Mechanisms controlling the interannual variability of sediment nitrogen cycling

To identify the drivers of interannual variations in sediment nitrogen cycling and nitrogen fluxes at the sediment–water interface, we conducted a series of sensitivity experiments in which each of seven interannually varying input variables was replaced by its climatological monthly mean, retaining only seasonal variability. The seven variables were sediment mineralization rate (Rm), bottom-water temperature (T^{bw}), and bottom-water concentrations of PON (PON^{bw}), NH_4^+ (NH_4^{+bw}), NO_2^- (NO_2^{-bw}), NO_3^- (NO_3^{-bw}) and DO (DO^{bw}). Results were compared with the control simulation to evaluate their effects on annual mean sediment inventories and sediment–water fluxes (Figure 6 and 7).

https://doi.org/10.5194/egusphere-2026-7013
Preprint. Discussion started: 20 November 2026
© Author(s) 2026. CC BY 4.0 License.

The sensitivity experiments reveal a hierarchical control of interannual sediment nitrogen cycling rather than dominance by a single forcing. PON^{bw}, Rm, DO^{bw}, and NO_3^{-bw} concentration were the dominant controlling variables, while the remaining factors exert comparatively minor influences. External forcing was propagated through a sequence of sediment processes, beginning with PON supply and accumulation, followed by mineralization and oxygen consumption, and ultimately affecting nitrification and nitrogen removal.

Sediment PON represents the largest nitrogen reservoir and the starting point of this propagation pathway. Its interannual variability reflects the balance between PON input and mineralization (Figure 6a). PON^{bw} concentration primarily controlled the sediment–water PON flux, as removing its interannual variability nearly eliminated the interannual variability of PON flux (Figure 7a), whereas Rm controlled PON mineralization (Figure S8a). Before 2010, relatively high PON^{bw} concentrations combined with relatively low mineralization rates resulted in PON deposition exceeding mineralization, leading to continuous PON accumulation. After 2010, declining PON deposition and enhanced mineralization reduced this imbalance, causing sediment PON inventory to fluctuate around a relatively stable level. The sediment PON mass balance further supports this interpretation (Figure S9a). Therefore, interannual evolution of sediment PON inventory reflects the long-term balance between external organic matter supply and internal degradation.

Mineralization transfers this variability to the dissolved nitrogen pool by converting sedimentary PON into NH_4^+. Accordingly, Rm was the primary control on sediment NH_4^+ inventory and NH_4^+ flux (Figure 6b and 7b). Because NH_4^+ concentrations near the sediment surface were consistently much higher than those in bottom water (Figures 2b and 4b), the NH_4^+ concentration gradient across the interface was mainly determined by sedimentary production. PON^{bw} concentration also indirectly affected NH_4^+ production by regulating PON supply. Thus, PON^{bw} concentration determines the substrate supply, whereas Rm regulates its conversion into NH_4^+.

DO availability links PON decomposition with subsequent nitrogen transformations. Mineralization is the major oxygen-consuming process, and both PON^{bw} concentration and Rm substantially affected sediment oxygen demand and the sediment–water DO flux (Figure 7c). Because DO enters the sediment mainly through diffusion from bottom water, DO^{bw} concentration additionally regulated sediment DO

https://doi.org/10.5194/egusphere-2026-7013
Preprint. Discussion started: 20 November 2026
© Author(s) 2026. CC BY 4.0 License.

inventory (Figure 6c). Therefore, sediment oxygen conditions emerged from the combined effects of external DO supply and internal DO consumption.

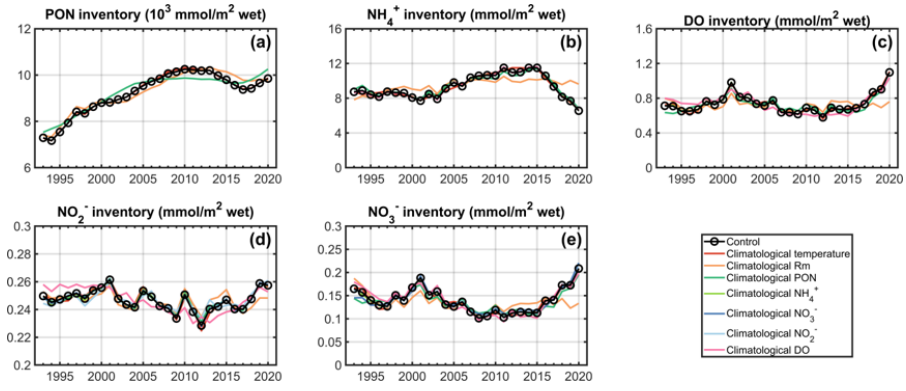


Figure 6. Comparisons of the sedimentary inventories among eight calculations (seven sensitivity experiments and one control run). The sensitivity experiments include the cases removing the interannual variations of water temperature (red, "Climatological temperature"), PON concentration (dark green, "Climatological PON"), NH_4^+ concentration (light green, "Climatological NH_4^+"), NO_3^- concentration (dark blue, "Climatological NO_3^-"), NO_2^- concentration (light blue, "Climatological NO_2^-"), and DO concentration (pink, "Climatological") in the overlying water, as well as of the mineralization rate (orange, "Climatological Rm"). (a) PON inventory; (b) NH_4^+ inventory; (c) DO inventory; (d) NO_2^- inventory; (e) NO_3^- inventory.

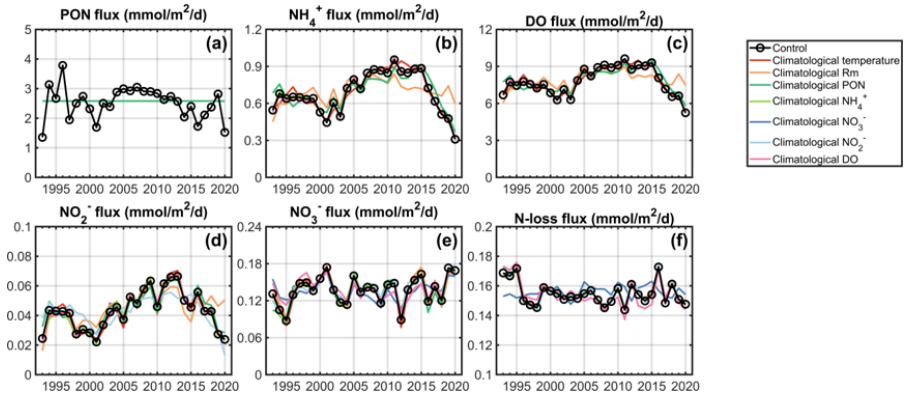


Figure 7. The same as Figure 6 but for the sediment-water interface fluxes in the eight calculations: (a) PON flux; (b) NH_4^+ flux; (c) DO flux; (d) NO_2^- flux; (e) NO_3^- flux; (f) N-loss flux.

The effects of PON supply, mineralization, and DO availability were subsequently propagated to oxidized nitrogen. Because nitrification is strongly DO dependent, sediment DO regulated the production of NO_2^- and NO_3^- (Figures S8b, c), making PON^{bw} concentration, Rm, and DO^{bw} concentration the dominant controls on their sediment inventories and fluxes (Figures 6d, e and 7d, e). NO_2^{-bw} and NO_3^{-bw} concentrations also directly influenced their concentration gradients across the interface and

https://doi.org/10.5194/egusphere-2026-7013
Preprint. Discussion started: 20 November 2026
© Author(s) 2026. CC BY 4.0 License.



therefore contribute to regulating their respective sediment inventories. Finally, NO_3^{-bw} concentration provided an additional constraint on nitrogen removal by regulating NO_3^- availability for denitrification (Figure S8d), whereas anammox was more strongly associated with sediment redox conditions and therefore controlled by DO^{bw} concentration (Figure S8f). Consequently, interannual variability in N-loss flux reflected the combined effects of NO_3^{-bw} and DO^{bw} concentration rather than a single forcing. Overall, these experiments demonstrate that interannual variability in sediment nitrogen cycling arises from coupled effects of external organic matter supply, organic matter reactivity, and sediment redox conditions. PON^{bw} controls PON supply, while Rm regulates its conversion to NH_4^+ and associated oxygen consumption. DO^{bw} controls external oxygen supply, allowing sediment redox conditions to propagate these effects to nitrification and nitrogen removal, while NO_3^{-bw} independently constrains denitrification. This hierarchical control framework provides the basis for interpreting the effects of long-term eutrophication and warming discussed below.

4.2 Eutrophication impacts on sediment nitrogen cycling

Bottom-water TN concentrations in Harima Nada were substantially higher during 1992–1996 than after 1997 (Figure 2a), with a mean concentration approximately 30% higher than during 1997–2020, indicating that the early 1990s represented a eutrophic phase. To isolate the effect of eutrophication, we constructed a non-eutrophic scenario by reducing bottom-water PON, NH_4^+, NO_2^- and NO_3^- concentrations by 30% during 1992–1996 while keeping all other forcing identical to the control simulation. Relative differences between the two simulations were used to quantify eutrophication impacts, with changes smaller than 5% considered negligible.

4.2.1 Mechanisms underlying eutrophication impacts

Eutrophication propagated through the sediment nitrogen cycle as a sequential process rather than an instantaneous response (Figure 8). Increased nutrient concentrations immediately enhanced PON deposition, whereas sediment inventories and some benthic fluxes responded more slowly because deposited organic matter accumulated and was remineralized over extended periods.

The immediate response occurred at the sediment-water interface: PON flux increased by 32% at the onset of eutrophication began (Figure 8f). Because mineralization was slower than deposition, much of

https://doi.org/10.5194/egusphere-2026-7013
Preprint. Discussion started: 20 November 2026
© Author(s) 2026. CC BY 4.0 License.

the additional organic matter was initially stored in the sediment. Consequently, the cumulative increase in PON inventory remained negligible during the first two years and become significant only after three years of sustained accumulation (Figure 8a). After eutrophication ended, the accumulated PON continued to decompose, producing a maximum inventory increase of 11% one year later and extending the influence of the 4.5-year eutrophication period by another 8 years.

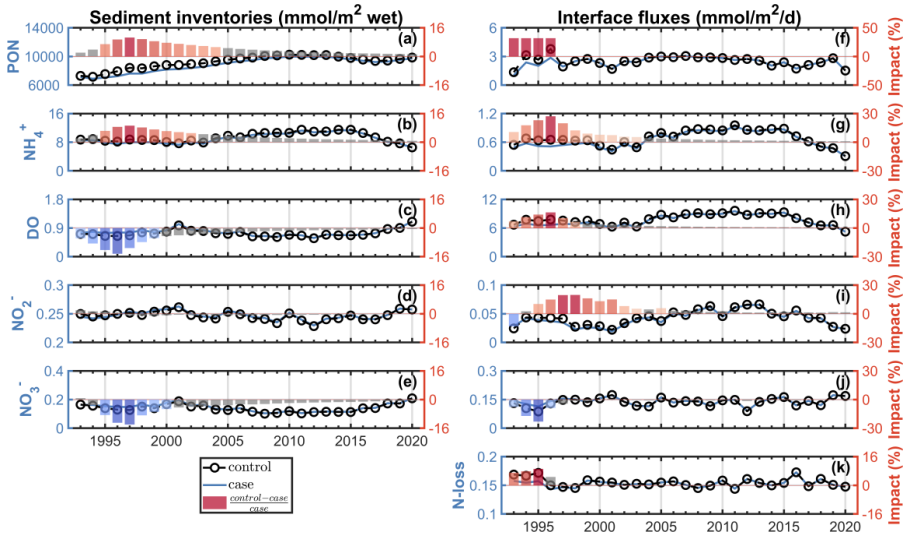


Figure 8. Comparisons of the model results between control run (eutrophic scenario) and non-eutrophic scenario: (a) PON inventory; (b) NH_4^+ inventory; (c) DO inventory; (d) NO_2^- inventory; (e) NO_3^- inventory; (f) PON flux; (g) NH_4^+ flux; (h) DO flux; (i) NO_2^- flux; (j) NO_3^- flux; (k) N-loss flux. The red bars indicate eutrophication effects exceeding 5%, the blue bars correspond to values below -5%, and the gray bars denote values with an absolute magnitude less than 5%.

This delayed remineralization propagated the eutrophication signal to other components of the nitrogen cycle. Sediment NH_4^+ inventory increased with a similar delay, reaching a maximum increase of 9% and remaining affected for six additional years (Figure 8b). In contrast, NH_4^+ flux responded immediately to enhanced mineralization, reaching a maximum increase of 27% and retaining a legacy for 7 years (Figure 8g). Increased mineralization also enhanced sediment oxygen demand, decreasing DO inventory by up to 14% and increasing oxygen uptake from bottom water by 16% (Figures 8c and 8h).

The resulting decline in DO altered nitrogen transformation pathways. NO_2^- inventory changed little because of its rapid turnover (Figure 8d), but its flux showed a two-stage response: an initial decrease caused by DO limitation of nitrification followed by an increased as continuous remineralization supplied

https://doi.org/10.5194/egusphere-2026-7013
Preprint. Discussion started: 20 November 2026
© Author(s) 2026. CC BY 4.0 License.

additional NH_4^+, reaching a maximum increase of 20% and persisting for 9 years after eutrophication ceased (Figure 8i). NO_3^- inventory responded similarly to DO inventory with an approximately one-year delay (Figure 8e). In contrast, NO_3^- flux and nitrogen removal exhibited little post-eutrophication legacy because they were primarily constrained by bottom-water NO_3^- concentrations (Figures 8j and 8k). Overall, the eutrophication legacy originated from the mismatch between rapid organic matter deposition and slower sediment remineralization. Interface fluxes responded rapidly to changes in external loading, whereas sediment inventories required sustained accumulation before becoming substantially altered and subsequently retained the eutrophication signal after external loading declined.

4.2.2 Controls on the magnitude and persistence of eutrophication impacts

We quantified eutrophication responses using maximum impact, representing the largest deviation from the non-eutrophic scenario, and additional impact years, representing the period after eutrophication during which the relative impact remained greater than 5%.

Increasing eutrophication duration from 1.5 to 7.5 years while maintaining the same nutrient enrichment generally prolonged legacy effects on sediment nitrogen inventories and fluxes (Figure 9a and S10). However, the increase in persistence gradually slowed when eutrophication lasted longer than approximately 4–5 years, indicating an upper limit to sediment memory. Maximum impacts showed a similar tendency (Figure 9b and S10). Variables closely associated with organic matter storage, particularly sedimentary PON and NH_4^+ inventories, continued to increase with eutrophication duration, whereas variables primarily controlled by external forcing, such as PON flux and NO_2^- inventory, changed little. Thus, prolonged eutrophication mainly amplifies the sediment memory. As organic matter continuously accumulates, sediment remineralization gradually approaches a new balance with deposition, and the extension of eutrophication duration produces progressively smaller increases in both impact magnitude and recovery time.

In contrast, varying bottom-water TN concentrations from 70% to 160% of the non-eutrophic level while fixing the eutrophication duration at 4.5 years produced an approximately linear increase in both additional impact years and maximum impacts (Figures 9c, d and S10). Stronger nutrient enrichment increased organic matter deposition and sediment storage, leading to proportionally larger changes in sediment nitrogen inventories and benthic fluxes. Unlike eutrophication duration, no saturation was

https://doi.org/10.5194/egusphere-2026-7013
Preprint. Discussion started: 20 November 2026
© Author(s) 2026. CC BY 4.0 License.

observed over the enrichment range examined, indicating that eutrophication severity primarily controls the amplitude of sediment biogeochemical responses.

Interestingly, oligotrophic conditions (−30% TN) produced responses that were nearly symmetrical to those under eutrophic conditions (+30% TN). Reduced nutrient loading decreased sediment organic matter storage and benthic nitrogen cycling, while the recovery times remained comparable. This symmetry suggests that sediments integrate changes in external nutrient loading over time, with the slow organic matter turnover extending the response beyond the duration of the initial perturbation.

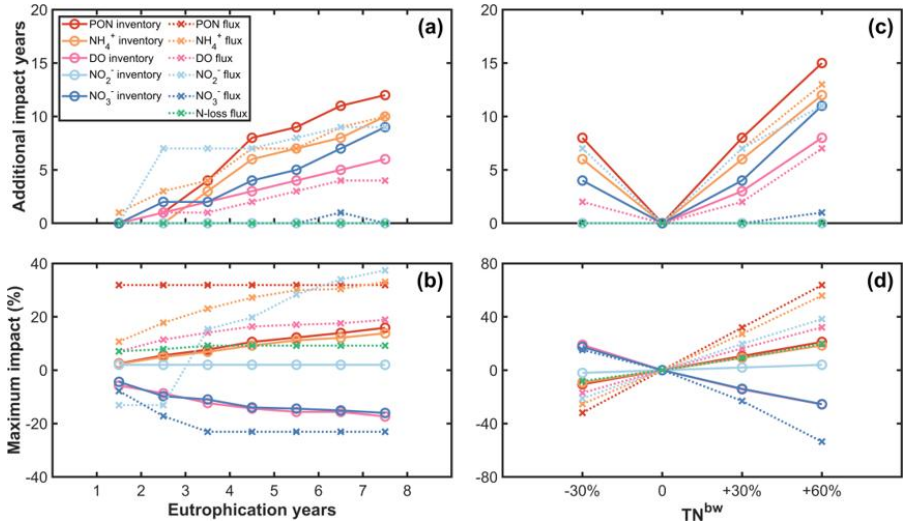


Figure 9. Sensitivity of sediment nitrogen inventories and sediment–water nitrogen fluxes to eutrophication duration and bottom-water total nitrogen (TN^{bw}) level. In the eutrophication-duration experiments (a, b), TN^{bw} concentration was fixed at 130% of the non-eutrophic level, while the duration varied from 1.5 to 7.5 years. In the TN^{bw}-level experiments (c, d), the perturbation duration was fixed at 4.5 years, while TN^{bw} varied from 70% to 160% of the non-eutrophic level, representing oligotrophic (70%) and eutrophic (130% and 160%) scenarios. (a) Additional impact years as a function of eutrophication duration. (b) Maximum impact as a function of eutrophication duration. (c) Additional impact years as a function of TN^{bw}-level. (d) Maximum impact as a function of TN^{bw}-level. Additional impact years are defined as the period after the imposed TN^{bw} perturbation ends during which the relative impact remains greater than 5%, and maximum impact represents the largest relative difference between the perturbed and non-eutrophic simulations.

Together, these experiments reveal two distinct response modes. Prolonging eutrophication primarily extends sediment memory, with persistence gradually approaching an upper limit, whereas increasing nutrient enrichment primarily amplifies the magnitude of the response in an approximately proportional manner. Thus, the persistence of eutrophication impacts is governed largely by the intrinsic processing

https://doi.org/10.5194/egusphere-2026-7013
Preprint. Discussion started: 20 November 2026
© Author(s) 2026. CC BY 4.0 License.

capacity of sediments, while their magnitude is more directly determined by the intensity of external nutrient enrichment.

4.3 Limited impact of seawater warming on sediment nitrogen cycling

Bottom-water temperatures in Harima Nada exhibited warming trends during autumn and winter from 1981 to 2020, at rates of 0.0472 and 0.0423 °C yr^{-1}, respectively (Figure S12). To isolate the effect of warming, these long-term trends were removed from the autumn and winter temperature records while preserving seasonal variability. The resulting no-warming simulation was compared with the control simulation, with relative changes below 5% considered negligible.

Seawater warming gradually accumulated its influence on sediment nitrogen cycling (Figure S13). Elevated bottom-water temperatures enhanced mineralization, causing slight decreases in PON and DO inventories and an increase in NH_4^+ inventory. Enhanced oxygen consumption also inhibited nitrification, leading to a small reduction in sediment NO_3^- inventory and modest increases in NH_4^+, NO_2^-, and DO fluxes across the sediment–water interface. Nevertheless, the relative impacts on all sediment nitrogen inventories and sediment–water fluxes remained below 5% throughout the 28-year simulation, indicating that seawater warming exerted only a minor influence on sediment nitrogen cycling in Harima Nada during this period.

The limited response primarily reflects the modest magnitude of warming rather than an intrinsic insensitivity of sediment nitrogen cycling to temperature. Although warming accelerates mineralization and can consequently alter oxygen consumption and nitrogen transformations, cumulative warming in Harima Nada during the study period was approximately 1.5 °C. This relatively small temperature increase therefore produced limited enhancement of mineralization and its cascading effects. Consistent with this interpretation, laboratory incubations reported weak responses of sediment nitrogen cycling to temperature increases below approximately 6 °C (Sanz-Lázaro et al., 2015).

The warming rate observed in Harima Nada is nevertheless comparable to upper-range warming projected under the high-emission scenario (RCP8.5). Global sea surface temperature under RCP8.5 was projected to increase at approximately 0.043 °C yr^{-1} (Cheng et al., 2019; Pörtner et al., 2019), comparable to the historical warming rate observed here. Therefore, the past three decades in Harima Nada may be regarded as a realistic analogue for the upper range of coastal warming expected over the coming decades.

https://doi.org/10.5194/egusphere-2026-7013
Preprint. Discussion started: 20 November 2026
© Author(s) 2026. CC BY 4.0 License.

Since this relatively rapid warming produced only negligible changes in sediment nitrogen cycling, seawater warming alone is unlikely to substantially alter sediment nitrogen cycling in most coastal regions over the next several decades.

Overall, our simulations indicate that eutrophication-related changes in nutrient loading were the dominant driver of long-term sediment nitrogen variability in Harima Nada, while the influence of seawater warming remained limited. The model is one-dimensional and therefore does not resolve spatial heterogeneity in sediment properties and benthic processes; the results primarily represent the central Harima Nada and basin-scale tendencies. In addition, direct observations of individual benthic nitrogen fluxes remain unavailable for independent validation, introducing uncertainty into quantitative estimates of individual nitrogen transformation pathways. Nevertheless, the model provides a process-based framework for linking long-term changes in bottom-water conditions to sediment nitrogen cycling. Future studies combining direct benthic flux measurements with spatially resolved models will be important for evaluating the generality of these mechanisms and constraining regional nitrogen budgets under future environmental change.

5. Conclusion

Using a one-dimensional sediment nitrogen cycling model constrained by long-term observations, we reconstructed the evolution of sediment nitrogen profiles and sediment–water nitrogen fluxes in Harima Nada from July 1992 to April 2021. The results provide a process-based assessment of how long-term environmental changes in the overlying water affect sediment nitrogen cycling in a semi-enclosed coastal sea.

The simulations reveal a hierarchical propagation of external forcing rather than by any single environmental factor. Bottom-water PON determines organic matter supply to the sediment, while sediment mineralization regulates its conversion to NH_4^+. Together, these processes determine sediment oxygen demand, whereas bottom-water DO controls external oxygen supply. Sediment DO availability subsequently mediates nitrification and nitrogen removal, while bottom-water NO_3^- independently constraints denitrification. Consequently, long-term variability in sediment nitrogen inventories,

https://doi.org/10.5194/egusphere-2026-7013
Preprint. Discussion started: 20 November 2026
© Author(s) 2026. CC BY 4.0 License.

sediment–water fluxes, and nitrogen loss emerges from the coupled effects of organic matter supply, its reactivity, microphytobenthos activity and sediment redox conditions.

The numerical experiments further demonstrate contrasting effects of eutrophication and seawater warming. Eutrophication enhances PON accumulation and sediment oxygen demand, generating legacy effects that persist for years after nutrient loading returns to normal because of the slow turnover of sediment PON. Extending the duration of eutrophication gradually lengthens and amplifies these impacts until the sediment system approaches a new balance between organic matter deposition and remineralization; increasing eutrophication intensity produces an approximately proportional increase in both impact magnitude and persistence. In contrast, the approximately 1.5 °C warming observed in Harima Nada over three decades produced only minor changes in sediment nitrogen inventories and sediment–water fluxes. Based on the long-term responses identified in Harima Nada, our results suggest that future changes in sediment nitrogen cycling in semi-enclosed coastal seas are likely to remain more strongly influenced by variations in nutrient loading than by the seawater warming expected over the coming decades.

The present model does not resolve spatial heterogeneity and lacks direct observations of individual benthic nitrogen fluxes and nitrogen removal rates for independent validation. It was also developed primarily for muddy sediments and does not explicitly represent porewater advection, which may be important in highly permeable sediments. Nevertheless, the model successfully reproduces observed long-term variations in sediment nitrogen concentrations and sediment–water fluxes, providing a process-based framework for investigating sediment nitrogen cycling in semi-enclosed coastal seas. Future development of a coupled water–sediment model with spatially resolved processes and improved observational constraints will help evaluate the spatial generality of these mechanisms.

Code, data, or code and data availability

Data will be made available on request.

https://doi.org/10.5194/egusphere-2026-7013
Preprint. Discussion started: 20 November 2026
© Author(s) 2026. CC BY 4.0 License.

Supporting Information

Supporting Information is available free of charge at the website.

Authorship contributions

Zhaosen Wu: Conceptualization, Methodology, Validation, Visualization, Writing – original draft. **Xinyu Guo:** Conceptualization, Funding acquisition, Methodology, Supervision, Writing – review & editing. **Masatoshi Nakakuni:** Data curation, Investigation, Resources. **Kuninao Tada:** Data curation, Investigation, Resources.

Declaration of competing interest

The authors declare that they have no known competing financial interests or personal relationships that could have appeared to influence the work reported in this paper.

Acknowledgement

This research was performed by the Environment Research and Technology Development Fund (JPMEERF20255002) of the Environmental Restoration and Conservation Agency provided by the Ministry of Environment of Japan. We thank Dr. Akihiko Morimoto and Dr. Naoki Yoshie who worked in the Center for Marine Environmental Studies, Ehime University, Japan and provided valuable suggestions for our research. Z. Wu thanks the China Scholarship Council (CSC) and the Ministry of Education, Culture, Sports, Science and Technology, Japan (MEXT) for a project on Joint Usage/Research Center, Leading Academia in Marine and Environmental Research (LaMer) for supporting his study in Japan.

https://doi.org/10.5194/egusphere-2026-7013
Preprint. Discussion started: 20 November 2026
© Author(s) 2026. CC BY 4.0 License.

References

Berner, R., 1980. Early diagenesis: a theoretical approach: Princeton. https://doi.org/10.1515/9780691209401.

Boynton, W.R., Ceballos, M.A.C., Bailey, E.M., Hodgkins, C.L.S., Humphrey, J.L., Testa, J.M., 2017. Oxygen and Nutrient Exchanges at the Sediment-Water Interface: a Global Synthesis and Critique of Estuarine and Coastal Data. Estuaries Coasts 41(2), 301-333. https://doi.org/10.1007/s12237-017-0275-5.

Cheng, L., Abraham, J., Hausfather, Z., Trenberth, K.E., 2019. How fast are the oceans warming? Science 363(6423), 128-129. https://doi.org/10.1126/science.aav7619.

Dai, Y., Yang, S., Zhao, D., Hu, C., Xu, W., Anderson, D.M., Li, Y., Song, X.-P., Boyce, D.G., Gibson, L., Zheng, C., Feng, L., 2023. Coastal phytoplankton blooms expand and intensify in the 21st century. Nature 615(7951), 280-284. https://doi.org/10.1038/s41586-023-05760-y.

Devol, A.H., 2015. Denitrification, Anammox, and N2 Production in Marine Sediments. Annu. Rev. Mar. Sci. 7(1), 403-423. https://doi.org/10.1146/annurev-marine-010213-135040.

Diaz, R.J., Rosenberg, R., 2008. Spreading Dead Zones and Consequences for Marine Ecosystems. Science 321(5891), 926-929. https://doi.org/10.1126/science.1156401.

Ding, X., Guo, X., Gao, H., Gao, J., Shi, J., Yu, X., Wu, Z., 2021. Seasonal variations of nutrient concentrations and their ratios in the central Bohai Sea. Sci Total Environ 799, 149416. https://doi.org/10.1016/j.scitotenv.2021.149416.

Ding, X., Shi, J., Guo, X., Gao, H., Liu, S., Guo, W., 2023. Interannual variations in the nutrient cycle in the central Bohai Sea in response to anthropogenic inputs. Chemosphere 313. https://doi.org/10.1016/j.chemosphere.2022.137620.

Han, A., Kao, S.J., Lin, W., Lin, Q., Han, L., Zou, W., Tan, E., Lai, Y., Ding, G., Lin, H., 2021. Nutrient Budget and Biogeochemical Dynamics in Sansha Bay, China: A Coastal Bay Affected by Intensive Mariculture. Journal of Geophysical Research: Biogeosciences 126(9). https://doi.org/10.1029/2020jg006220.

Hayashi, M., 2001. The study of lower trophic level ecosystem and construction of the prediction model of the Seto Inland Sea. Nissan Science Foundation Research Report, p. 24.

https://doi.org/10.5194/egusphere-2026-7013
Preprint. Discussion started: 20 November 2026
© Author(s) 2026. CC BY 4.0 License.



590 Hedges, J.I., Stern, J.H., 1984. Carbon and nitrogen determinations of carbonate-containing solids.
591 Limnology and Oceanography 29(3), 657-663. https://doi.org/10.4319/lo.1984.29.3.0657.
592 Huang, F., Lin, X., Hu, W., Zeng, F., He, L., Yin, K., 2021. Nitrogen cycling processes in sediments of
593 the Pearl River Estuary: Spatial variations, controlling factors, and environmental implications.
594 CATENA 206, 105545. https://doi.org/10.1016/j.catena.2021.105545.
595 Ichimi, K., Tada, K., Montani, S., 2005. The phytoplankton assemblage of the past and present in the
596 Seto Inland Sea-the expectation from sediment core samples. Aquabiology 27, 214-221.
597 Ishii, D., Yanagi, T., Sasakura, S., 2014. Long-term trends in the occurrence of red tides in the Seto
598 Inland Sea, Japan. Oceanography in Japan 23(6), 217-236. https://doi.org/10.5928/kaiyou.23.6_217.
599 Itakura, S., Yamaguchi, M., 2007. Environmental Change and Occurrence Mechanism of Harmful Algal
600 Blooms in the Seto Inland Sea. Japanese journal of benthology 62, 57-61.
601 https://doi.org/10.5179/benthos.62.57.
602 Kamiyama, T., Tsujino, M., Tamai, K., 1998. Estimation of bottom fluxes of several nutrients in Harima
603 Nada, the Seto Inland Sea of Japan. Bulletin of the Nansei National Fisheries Research Institute
604 (Japan)(31).
605 Leng, Q., Guo, X., Zhu, J., Morimoto, A., 2023. Contribution of the open ocean to the nutrient and
606 phytoplankton inventory in a semi-enclosed coastal sea. Biogeosciences 20(20), 4323-4338.
607 https://doi.org/10.5194/bg-20-4323-2023.
608 Lønborg, C., Markager, S., 2021. Nitrogen in the Baltic Sea: Long-term trends, a budget and decadal
609 time lags in responses to declining inputs. Estuarine, Coastal and Shelf Science 261, 107529.
610 https://doi.org/10.1016/j.ecss.2021.107529.
611 Nakakuni, M., Loassachan, N., Ichimi, K., Nagao, S., Tada, K., 2022. Biophilic elements in core
612 sediments as records of coastal eutrophication in the Seto Inland Sea, Japan. Regional Studies in Marine
613 Science 50. https://doi.org/10.1016/j.rsma.2021.102093.
614 Nakakuni, M., Yamaguchi, H., Ichimi, K., Tada, K., 2024. Seasonal variation in pore water nutrients and
615 their fluxes from the bottom sediments in Harima Nada, Seto Inland Sea. Journal of Oceanography 80(3),
616 219-232. https://doi.org/10.1007/s10872-024-00719-7.

https://doi.org/10.5194/egusphere-2026-7013
Preprint. Discussion started: 20 November 2026
© Author(s) 2026. CC BY 4.0 License.



617 Nakakuni, M., Yamaguchi, H., Kimura, K., Nagare, C., Ichimi, K., Nii, T., Tada, K., 2026. Sustained
618 phytoplankton productivity despite declining dissolved inorganic nitrogen levels in Harima-Nada,
619 eastern Seto Inland Sea, Japan. Cell Reports Sustainability 3(7).
620 https://doi.org/10.1016/j.crsus.2026.100732.
621 Nishijima, W., Umehara, A., Okuda, T., Nakai, S., 2015. Variations in macrobenthic community
622 structures in relation to environmental variables in the Seto Inland Sea, Japan. Mar. Pollut. Bull. 92(1-
623 2), 90-98. https://doi.org/10.1016/j.marpolbul.2014.12.051.
624 Nishikawa, T., Hori, Y., Nagai, S., Miyahara, K., Nakamura, Y., Harada, K., Tanda, M., Manabe, T.,
625 Tada, K., 2009. Nutrient and Phytoplankton Dynamics in Harima-Nada, Eastern Seto Inland Sea, Japan
626 During a 35-Year Period from 1973 to 2007. Estuaries and Coasts 33(2), 417-427.
627 https://doi.org/10.1007/s12237-009-9198-0.
628 Oliver, K.I.C., Hoogakker, B.A.A., Crowhurst, S., Henderson, G.M., Rickaby, R.E.M., Edwards, N.R.,
629 Elderfield, H., 2010. A synthesis of marine sediment core δ13C data over the last 150 000 years. Clim
630 Past 6(5), 645-673. https://doi.org/10.5194/cp-6-645-2010.
631 Pörtner, H.-O., Roberts, D.C., Masson-Delmotte, V., Zhai, P., Tignor, M., Poloczanska, E., Weyer, N.,
632 2019. The ocean and cryosphere in a changing climate. IPCC special report on the ocean and cryosphere
633 in a changing climate 1155, 10.1017.
634 Sanz-Lázaro, C., Valdemarsen, T., Holmer, M., 2015. Effects of temperature and organic pollution on
635 nutrient cycling in marine sediments. Biogeosciences 12(15), 4565-4575. https://doi.org/10.5194/bg-12-
636 4565-2015.
637 Sayama, M., Sohma, A., Takasugi, Y., 2002. Experimental analysis of the effect of flow velocity on
638 oxygen dynamics near the water-sediment interface in a coastal zone. Proceedings of Coastal
639 Engineering 49, 996-1000. https://doi.org/10.2208/proce1989.49.996.
640 Soetaert, K., Herman, P.M.J., Middelburg, J.J., 1996. A model of early diagenetic processes from the
641 shelf to abyssal depths. Geochim. Cosmochim. Acta 60(6), 1019-1040. https://doi.org/10.1016/0016-
642 7037(96)00013-0.

https://doi.org/10.5194/egusphere-2026-7013
Preprint. Discussion started: 20 November 2026
© Author(s) 2026. CC BY 4.0 License.



643 Soetaert, K., Middelburg, J.J., 2009. Modeling eutrophication and oligotrophication of shallow-water
644 marine systems: the importance of sediments under stratified and well-mixed conditions. Hydrobiologia
645 629(1), 239-254. https://doi.org/10.1007/s10750-009-9777-x.
646 Strickland, J., Parsons, T., (1972). A practical hand book of seawater analysis-Ottawa. Fisheries Research
647 Board of Canada. 310p.
648 Tada, K., Montani, S., 1997. An Evaluation of Phosphate Upward Fluxes from the Coastal Sediments by
649 Three Different Methods. Fisheries science 63(4), 567-572. https://doi.org/10.2331/fishsci.63.567.
650 Tong-u-dom, S., Morimoto, A., Leng, Q., Guo, X., 2023. Seasonal variation in the current field and
651 development of bottom cold water in Harima-Nada. Journal of Oceanography 80(1), 1-20.
652 https://doi.org/10.1007/s10872-023-00702-8.
653 Tsujino, M., 2018. Biomass and production of macrobenthos in the Seto Inland Sea Japan. Nippon Suisan
654 Gakkaishi 84(2), 211-220. https://doi.org/10.2331/suisan.17-00042.
655 Wu, Z., Guo, X., Shi, J., Ding, X., Nakakuni, M., Tada, K., 2026. Seasonal variations and controlling
656 factors of nitrogen fluxes at the sediment-water interface in a semi-enclosed inland sea. Biogeosciences
657 23(17), 6053-6072. https://doi.org/10.5194/bg-23-6053-2026.
658 Yamaguchi, H., Hirade, N., Kayama, M., Ichimi, K., Tada, K., 2014. Total organic carbon and nitrogen
659 contents in surface sediments of Harima Nada, eastern Seto Inland Sea, Japan: a comparison under two
660 different trophic states. Journal of Oceanography 70(4), 355-366. https://doi.org/10.1007/s10872-014-
661 0235-7.
662 Yamamoto, T., Matsuda, O., Hashimoto, T., Imose, H., Kitamura, T., 1998. Estimation of benthic fluxes
663 of dissolved inorganic nitrogen and phosphorus from sediments of the Seto Inland Sea. Umi no Kenkyu
664 7, 151-158.
665 Yamamoto, T., Orimoto, K., Asaoka, S., Yamamoto, H., Onodera, S.-i., 2021. A Conflict between the
666 Legacy of Eutrophication and Cultural Oligotrophication in Hiroshima Bay. Oceans 2(3), 546-565.
667 https://doi.org/10.3390/oceans2030031.
668 Zhu, J., Guo, X., Shi, J., Gao, H., 2019. Dilution characteristics of riverine input contaminants in the Seto
669 Inland Sea. Mar. Pollut. Bull. 141, 91-103. https://doi.org/10.1016/j.marpolbul.2019.02.029.